Evaluation of the Role of System Matrix in SPECT Images Reconstructed by OSEM Technique

Mohsen Hajizadeh, PhD[1]; Seyed Rasoul Zakavi, MD[2];
Mehdi Momen-Nejad[1], PhD; Maryam Naji, Msc[3]

[1]Medical Physics Research Center, [2]Department of Nuclear Medicine, Imam Reza Hospital,
[3]Department of Medical Physics, Mashhad University of Medical Sciences, Mashhad, Iran.

ABSTRACT

Introduction: Ordered subset expectation maximization (OSEM), is an effective iterative method for SPECT image reconstruction. The aim of this study is the evaluation of the role of system matrix in OSEM image reconstruction method using four different physical beam radiation models with three detection configurations.

Methods: SPECT was done with an arc of 180 degree in 32 projections after injection of 2 mCi of ^{99m}Tc-pertechnetate in a heart phantom by a Siemens E.Cam gamma camera equipped with LEHR collimator and data were transferred to a PC computer for reconstruction of the images with Mathlab software. The system or probability matrixes were firstly calculated using radiation fraction of pixels for three different detection models with linear, rectangular and divergent FOV, and reduction coefficient of photons from pixels to detectors in four different radiation models of distance independent (DID), inverse distance dependence (IDD) [$\cong 1/R$], inverse square distance dependence (ISDD),[$\cong 1/R^2$] and inverse exponential distance dependence(IEDD),[$\cong exp\text{-}R$]. In these calculations the detector was assumed at a distance of 842 mm from the phantom center and pixel size was 6.638 mm. The divergent angle in divergent field of view was 2.08 degree. 12 Images of the phantom were reconstructed using system matrixes of 4 different radiation and 3 detection models. Qualities of the images were compared using universal image quality index, UIQI.

Results: The results shows negligible although statistically significant difference between contrast and brightness of the images, but it is possible in the organs with constant absorption coefficients such as brain, to use the system matrix with mathematical IEDD radiation model for attenuation correction in SPECT images. It is shown that variation in distance weighting factors in mathematical IEDD radiation model changes the system matrix so that the weights of deeper data decrease in image reconstruction process. Therefore, by this method contrast of the image at different depth can be controlled.

Conclusions: Applying different beam radiation models and detection configurations in system matrix has no significant improvements on the image quality. However image contrast at different depth can be controlled by using system matrix derived from different distance weighting factor in mathematical IEDD radiation model.

Key words: System matrix, SPECT, OSEM.

Corresponding author: Dr Mohsen Hajizadeh, Medical Physics Research Center, Mashhad University of Medical Sciences, Mashhad, Iran.   Email: hajizadeh@mums.ac.ir

INTRODUCTION

Nuclear medicine imaging is based on the administration of a gamma emitter labeled pharmaceuticals to a subject and an external device, the gamma camera, detects the distributed radioactivity in the body, from 1 or several angles of views. As it is impossible to determine the activity distribution through the body from only 1 projection, an image of a tomographic slice through the body can be obtained by acquiring projections over a large number of views around the subject, the basic idea of SPECT(1).

There are many different algorithms for SPECT image reconstruction, using either analytic or iterative techniques, such as filtered back-projection (FBP), conjugate gradient (CG), maximum likelihood expectation maximization (MLEM), which are pointed out by Kunyansky (2). Analytic image reconstructions such as filtered back-projection represent an exact mathematic solution. Although this algorithm is a relatively efficient operation, it does not always perform well on noisy projections and, as is the case with SPECT data, it generates artifacts when the projections are not line integrals of the internal activity (3). Iterative algorithms are a preferred alternate method for performing SPECT reconstruction, and over the past 5 years there has been a shift from filtered back-projection to iterative reconstruction in most clinics (4-6). The most efficient approach of iterative techniques is the Ordered Subset Expectation Maximization (OSEM), which has been proposed by Hudson and Larkin (7) to accelerate the reconstruction process with a small number of iterations.

An advantage of the iterative approach is that accurate corrections can be made for all physical properties of the imaging system (which may include physics of the radiation and detection geometry), and the attenuation, scatter and blurring effects in the reconstruction process(8).

The purpose of this work is to evaluate the role of system matrix in OSEM image reconstruction method, using four different physical beam radiation models with three detection configurations.

METHODS

The Iterative Reconstruction Algorithms in SPECT is based on the solution of g= Af, where g is the measured gamma camera data values in the sinogram, A is a given matrix called " system matrix", and f is the pixel values in the slice image of interest to be reconstructed. By assuming number of disintegrations and their detections as two Poisson independent variables , the MLEM algorithm as described by Lange and Carson(9) leads to the equation 1:

Eq. 1
$$f_j^{k+1} = \frac{f_j^k}{\sum_{i=1}^I a_{i,j}} \sum_i \frac{g_i}{\sum_{i=1}^I a_{i,j} f_j^k} a_{i,j}$$

Where g_i and $a_{i,j}$ are the sinogram measured data and elements of the system matrix respectively. The first image $f^{(0)}$ can be a uniform disk enclosed in the field of view (10) or an image obtained by FBP. The goal of the MLEM or OSEM algorithm is to find a "general" solution as the best estimate for f: the mean number of radioactive disintegrations in the image that can produce the sinogram g with the highest likelihood (9, 11). The EM algorithm can be seen as a set of successive projections/back-projections (12). In other words, at each iteration k, a system model (which may include physics of the radiation and detection geometry), will be used to simulate projections which then compared with the measured ones. Results are used to produce an updated (and hopefully more accurate) estimate, which becomes iteration k +1. To approach the final image, this process is repeated predefined times or should fulfill the stopping criteria.

To evaluate the importance and role of system matrix configuration on SPECT image reconstruction, we firstly calculate the system matrix elements of four different physical radiation model and three detection configurations, using Matlab software. Then SPECT was performed from a heart and chest phantom after injection of 2mCi of ^{99m}Tc pertechnetate inside the phantom (Figure 1).
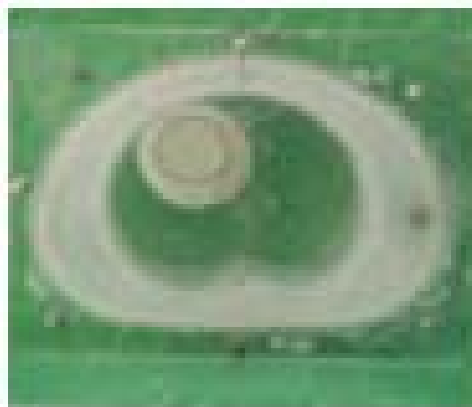

Fig 1: Transverse section of the heart and chest phantom composed of four cylinders, 15 cm long, which separates the internal heart, heart wall, lung and body-contour.

The technique which is used for acquisition was 32 projections at 180 degree around the phantom using a matrix of 64×64 pixels. The phantom which were made of 4 cylinders as shown in figure 1, were filled with water, except in spaces for lungs, and radiotracer is added in the heart wall and body contour. SPECT images were acquired by Siemens E.Cam gamma camera and were transferred in Dicam format to a pc computer as a three dimension matrix with 64×64×32 elements.

The system matrix (13) or probability matrix (14) is constructed from detection probability of the emissions received from different voxels in a defined slice of the subject by gamma camera at different position around that. This matrix, based on the physical radiation model of the beam, collimator specification and radiation detection geometry of gamma camera, can be calculated for a defined slice and is used in image reconstruction for all slices. Three different radiation detection geometry of linear, rectangular and divergent field of view, are shown in figure 2a. it is supposed that only photons that emits perpendicular to gamma camera surface can be received by detectors, therefore, at linear, rectangular and divergent detection models as shown in figure 2b, the fraction of emitted radiation from pixels received by gamma camera are proportional to the size of line through the pixels or surface of that which are in the detection field of view.

System matrix elements ($a_{i,j}$), which is detection probability of emitted photons from voxel i in a defined slice of subject at j detector on gamma camera surface, can be calculated from radiation fraction of pixels and reduction coefficient of photons from pixels to detector surface.

$a_{i,j}$ = radiation fraction of pixel i × reduction of photons along to detector j   Eq. 2

The first term, radiation fractions of pixels depend on the collimator design and detection model of photons and the second term is based on radiation model of photons. The system matrix A, for a SPECT image using 32 projections with 64×64 pixels, is a two dimension m×n matrix, which m=64×64=4096, is the number of image pixels and n=32×64=2048 is the number of detectors around the subject as a detection bin.

In order to calculate these system matrix elements, radiation fraction of pixels were firstly calculated for three detection models with linear, rectangular and divergent FOV, and then by ignoring attenuation of radiation in the subject, reduction coefficient of

photons from pixels to detectors in four different radiation models, with a distance independent (DID), inverse distance dependence (IDD) ($\cong 1/R$), inverse square distance dependence (ISDD) ($\cong 1/R2$) and inverse exponential distance dependence (IEDD) ($\cong exp-R$) were calculated. Finally 12 images of the phantom with OSEM technique were reconstructed using three system matrixes of different radiation and detection models.

Qualities of the images were compared using universal image quality index (UIQI).

RESULTS AND DISCUSSION

Images of the heart phantom with OSEM technique were reconstructed; using the system matrix based on the different radiation and detection models and is shown in figure 3. In these images the row data were acquired with a gamma camera 842 mm away from the phantom center equipped with a LEHR parallel whole collimator. Pixel size in the image was 6.638 mm, based on the detector size (616 mm) and matrix used for acquisition (64 × 64) and zoom of 1.45. The divergent angle in divergent field of view was 2.08 degree.

Comparison of the images were performed by three components of the UIQI index, the correlation between images and the similarity of the brightness and contrast (15). These components were calculated for all images while selecting the image reconstructed by rectangular FOV and DID radiation model as a standard image and unified the scale of the images by dividing pixel values of each image by its maximum value. Results were shown in table 1.

One way ANOVA analyses of the data show that, with 95% confidence interval, differences in brightness and contrast between radiations models are not significant (P>0.8) but it is significant for detection models(p<0.001). Using Tukey's Honestly significant test as a post-hot test, it also shows that difference between L (Linear) and R (Rectangular) detection models is not significant (P>0.8) and only differences between D (Divergent) with L and R detection models are statistically significant (P<0.002) which is due to more pixels coming to detector field in images reconstructed by divergent FOV.

 Therefore, we can conclude that although there are significant differences between D with L and R detection model, but values of the UIQI index and its component show that differences between contrast and brightness in the images are negligible.

Fig 2: Three different beam detection geometry for gamma camera, A) linear, rectangular and divergent field of view, B) Radiation fraction of pixels
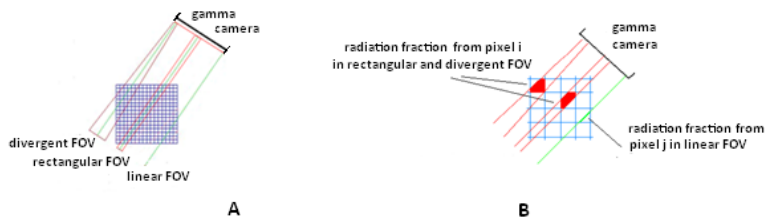
Radiation model \ Detection model	Linear FOV	Rectangular FOV	Divergent FOV
Distance independence (DID)			
Inverse distance dependence (IDD)			
Inverse square distance dependence (ISDD)			
Inverse exponential distance dependence (IEDD)			

Fig 3: images of the heart phantom with OSEM technique, using different radiation and detection models

$d_w = 0.05$	$d_w = 0.1$	$d_w = 0.15$	$d_w = 0.2$	$d_w = 0.25$
$d_w = -0.05$	$d_w = -0.1$	$d_w = -0.15$	$d_w = -0.2$	$d_w = -0.25$

Fig 4: Images of the heart phantom with rectangular FOV and IEDD mathematical radiation model, change of distance weighting factor, d_w, will change the image contrast in different depth.

This conclusion is confirmed by report of Glick et al (16) who have studied the attenuation with distance and detector response.

Table 1: UIQI index and its component for images reconstructed by different detection and radiation models.

No.	UIQI	Brightness	Contrast	Detection	Radiation
1	0.9989	0.9999	0.9999	L	DID
2	1	1	1	R	DID
3	0.9887	0.9949	0.9974	D	DID
4	0.9952	0.9988	0.9992	L	IDD
5	0.9974	0.9995	0.9997	R	IDD
6	0.9778	0.9903	0.9939	D	IDD
7	0.9869	0.9963	0.9979	L	ISDD
8	0.9912	0.9982	0.9991	R	ISDD
9	0.9776	0.9915	0.9942	D	ISDD
10	0.9988	0.9997	0.9998	L	EIDD
11	0.9996	0.9999	0.9999	R	EIDD
12	0.9771	0.9897	0.9934	D	EIDD

The IEDD would approach to DID model for $\mu=0$, therefore in figure 3, μ was 0.01 pixel^{-1} which is equal to 0.015 cm^{-1} the attenuation coefficient of air. As the attenuation of radiation in the subject is exponential and depends on the absorption coefficient and distance, i.e. $\exp(-\mu.r)$, it is possible in the subjects with constant absorption coefficients such as brain, to use the system matrix with mathematical IEDD radiation model for attenuation correction in SPECT images.

It is also possible to vary the weight (or coefficient) of distances in the model to vary the weight of deeper pixel in the image. In this case the radiation detection probability from deep pixels would vary and hence changes the contrast of the image in different depth. Images of the heart phantom with rectangular FOV and IEDD mathematical radiation model with different distance weighting factors of d_w, as $\exp(-d_w.R)$, are shown in figure 4. R is the distance of pixels from detectors.

In this model of radiation it is expected that variation in distance weighting factors changes the system matrix so that the weights of deeper data decrease in image reconstruction process. This leads to an image from surface voxels (with shorter distance to gamma camera) to be reconstructed, as shown in figure 4. Therefore, by this method contrast of the image at different depth can be controlled. This can be used to suppress a hot spot or high activity in part of an image and highlight the contrast of the other parts.

In figure 4, contrast of heart wall in the image with distance weighting factor of -0.1 (d_w=-0.1) is higher

than initial image (d_w=0). This can be seen from variations of UIQI index of these images as shown in figure 5. The largest variation of UIQI index are shown in 20-25 pixels image windows, which is almost the size of heart wall.
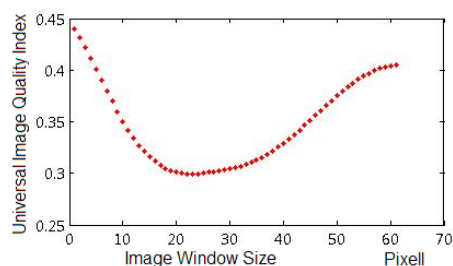

Fig 5: Variation of UIQI index in relation to window size for an image with distance weighting factor of -0.1 and initial image (d_w=0).

Also this method has the potential for application in ^{131}I SPECT in thyroid cancer patients, to improve the poor body contour in these images.

CONCLUSION

We conclude that the system matrix has an important role in OSEM image reconstruction. Although applying different beam radiation models in system matrix has no significant effect on the image quality, however linear and rectangular detection models at least theoretically have significantly improved the quality of images and it may be possible in the organs with constant absorption coefficients such as brain, to use the system matrix with mathematical IEDD radiation model for attenuation correction in SPECT images. Image contrast at different depth can also be controlled by different system matrix derived from different distance weighting factor in mathematical IEDD radiation model.

AKNOWLEDGEMENT

REFERENCES

1. Brooks RA, Di Chiro G. Principles of computer assisted tomography (CAT) in radiographic and radioisotopic imaging. Phys Med Biol 1976;21:689-732.

2. Kunyansky LA. A new SPECT reconstruction algorithm based on the Novikov explicit inversion formula Inverse Problems, . 2001;17(2):293-306.

3. Bruyant PP. Analytic and iterative reconstruction algorithm in SPECT. J Nucl Med. Oct. 2002;43(10):1343-58.

4. Lalush DA, Wernick MN. Emission Tomography: The Fundamentals of SPECT and PET. 1 st ed. Wernick MN, Aarsvold JN, editors. San Diego, CA.: Elsevier; 2004.

5. Qi J, Leahy RM. Iterative reconstruction techniques in emission computed tomography. Phys Med Biol. 2006;51:541-78.

6. Defrise M, Gullberg GT. Image reconstruction. Phys Med Biol 2006;51:139-54.

7. Hudson HM, Larkin RS. Accelerated image reconstruction using ordered subsets of projection data. . IEEE Trans Med Imaging 1994;13:601–9.

8. Gourion D, Noll D, Gantet P, Celler A, Esquerre J.P. Attenuation correction using SPECT emission data only. IEEE Trans Nucl Sci. 2002;49(5):2172-9.

9. Lange K, Carson R. EM reconstruction algorithms for emission and transmission tomography J Comput Assist Tomogr. 1984;8:306–16.

10. Llacer J, Veklerov E, Coakley K, Hoffman E, Nunez J. Statistical analysis of maximum likelihood estimator images of human brain FDG PET studies. IEEE Trans Med Imaging 1993;12:215–31.

11. Shepp LA, Vardi Y. Maximum likelihood reconstruction for emission tomography. IEEE Trans Med Imaging Ml-1. 1982:113–22.

12. Green PJ. Bayesian reconstructions from emission tomography data using a modified EM algorithm. IEEE Trans Med Imaging 1990;9:84–93.

13. Fessler J. Iterative methods for image reconstruction. ISBI tutorial, Arlington Virginia. April 2006.

14. Larson A. Corrections for improvement quantitative accuracy in planar scintigraphy and SPECT. PhD thesis Ũmea university, Sweden. 2006.

15. Wang Z, Bovik AC. A Universal Image Quality Index,. IEEE, Signal Processing Letters,. Mar 2002;9(3): 81-4.

16. Glick SJ, Penney BC, King MA, Byrne CL. Noniterative compensation for the distance-dependent detectorresponse and photon attenuation in SPECT imaging. IEEE Trans Med Imaging. Jun 1994;13(2):363-74.